

NMR study of the diluted magnetic semiconductor alloys $\text{Cd}_{1-x}\text{Mn}_x\text{Se}$, $\text{Cd}_{1-x}\text{Co}_x\text{Se}$, and $\text{Cd}_{1-x}\text{Fe}_x\text{Se}$

V. Ladizhansky, A. Faraggi, V. Lyahovitskaya, and S. Vega

Department of Chemical Physics, Weizmann Institute of Science, 76100 Rehovot, Israel

(Received 18 February 1997)

Diluted magnetic semiconductors $\text{Cd}_{1-x}\text{Mn}_x\text{Se}$ for $x=0.01$, $\text{Cd}_{1-x}\text{Fe}_x\text{Se}$ for $x=0.01$ and 0.02 , and $\text{Cd}_{1-x}\text{Co}_x\text{Se}$ for $x=0.006$, 0.009 , and 0.01 were studied in the temperature range of 180–400 K by ^{113}Cd magic-angle-spinning NMR spectroscopy. The NMR spectra of $\text{Cd}_{1-x}\text{Fe}_x\text{Se}$ and $\text{Cd}_{1-x}\text{Co}_x\text{Se}$ contain a set of resonance lines that are shifted away from the line of the undoped CdSe compound by the transferred hyperfine (THF) interaction between the cadmium nuclei and the paramagnetic ions. The temperature dependence of the THF shifts follows the Curie-Weiss law, and the spin-lattice relaxation times of the shifted lines are significantly shorter than that of the CdSe line. The ^{113}Cd lines show anisotropies that are smaller than the values evaluated from the dipolar interaction between the paramagnetic ions (M) and their nearest-neighboring cations (M -Se-Cd). The detected anisotropies are therefore composed of dipolar and hyperfine contributions from next-nearest-neighboring (NNN) cadmium nuclei (M -Se-Cd-Se-Cd). The spin-lattice relaxation times of the spectral lines are determined by the electron-nuclear dipolar interaction with NNN cations. The number of observed lines corresponds to the number of nonequivalent NNN cations around each paramagnetic ion. Using the values of the relaxation times and the amplitudes of the lines, it is possible to correlate each line to a well-defined NNN conformation. The NMR spectra of $\text{Cd}_{1-x}\text{Mn}_x\text{Se}$ did not show any fine structure similar to that observed in the Co and Fe alloys. [S0163-1829(97)06735-0]

I. INTRODUCTION

Diluted magnetic semiconductors (DMS's) of the form $A_{1-x}^{II}M_xB^{VI}$, with cations $A^{II}=\text{Cd}^{2+}$, Zn^{2+} , and Hg^{2+} , anions $B^{VI}=\text{Se}^{2-}$, Te^{2-} , and S^{2-} , and $M=\text{Mn}^{2+}$, Co^{2+} , and Fe^{2+} substituting part of the cations, have received considerable attention in recent years.¹⁻⁴ The lattice constants and band parameters of these ternary DMS alloys can be modified by varying the concentration of the paramagnetic impurities. The presence of the paramagnetic ions can yield interesting magnetic properties.^{2,4-10} For example, large concentrations of paramagnetic impurities result at low temperatures in the formation of spin-glass-like states.^{11,12} These and other magnetic properties are related to long-range exchange (superexchange) interactions that are mediated by the spin polarization of the electron density distributions between the paramagnetic ions. The magnitudes of these interactions are strongly dependent on the lengths and angles and on the covalence strengths and the orbital hybridizations of the bonds connecting the paramagnetic impurities.^{13,14}

Another type of magnetic interaction that exists in the DMS alloys is the transferred hyperfine (THF) interaction between the unpaired electrons of the magnetic ions and the nuclear spins of the nonmagnetic atoms. This interaction can be monitored by NMR spectroscopy. Since the THF interaction is also mediated by spin polarization of electronic orbitals, a better understanding of the dependence of this interaction on the bond properties of the interacting atoms can provide information about the electronic mechanism governing the superexchange.

The transferred hyperfine interactions in the alloys $\text{Cd}_{1-x}\text{Mn}_x\text{Te}$ (Ref. 15) and $\text{Cd}_{1-x}\text{Fe}_x\text{Te}$ (Ref. 16), exhibiting a zinc-blende structure, have already been studied by

^{113}Cd NMR. It was shown that the different lines in the ^{113}Cd NMR spectra of these alloys correspond to cadmium atoms that are differently coordinated to a paramagnetic ion and therefore experience different THF interactions. Interactions with nearest-neighbor (NN) and next-nearest-neighbor (NNN) cadmium atoms could be distinguished.

Here we report the results of a ^{113}Cd NMR study of the $\text{Cd}_{1-x}\text{Mn}_x\text{Se}$, $\text{Cd}_{1-x}\text{Fe}_x\text{Se}$, and $\text{Cd}_{1-x}\text{Co}_x\text{Se}$ alloys, possessing a wurtzite structure.⁴ The zinc-blende structure is cubic, whereas the wurtzite structure is hexagonal. In the zinc-blende and wurtzite crystals, a paramagnetic ion, replacing a cadmium ion in the lattice, has 12 NN cations, located at sites that are two bonds (M - B^{VI} -Cd) away. In the zinc-blende structure the 12 NN sites are all related crystallographically. In the wurtzite three sets of sites, not related by crystal symmetry, can be distinguished: 6 "in-plane" sites, 3 "above-the-plane" sites, and 3 "below-the-plane" sites. The 12 cadmium atoms at these sites are all equidistant to the central ion.

The zinc-blende and wurtzite structures differ significantly, when the bond structures between a center ion and its NNN cations are considered. The 42 NNN atoms in the zinc-blende lattice can be classified according to 4 nonequivalent bond structures. They can be characterized by *trans-trans* (*tt*), *gauche-trans* (*gt*), *trans-gauche* (*tg*), and *gauche-gauche* (*gg*) conformations.¹⁶ In the wurtzite structure there are 44 NNN cadmium atoms, which must be divided into 11 conformations. Each conformation is characterized by four bonds (M -Se-Cd-Se-Cd) and can be defined by the dihedral angles of the third and fourth bonds starting from M . In this terminology the *tg* conformation is assigned by (180°, 60°) and the *tt* conformation by (180°, 180°). Table I summarizes the 4 sets of NNN cadmium sites in the zinc-blende structure

TABLE I. Bond conformations, number of sites, and distances between the paramagnetic ion (M) and the cadmium atoms of NNN cation configurations in wurtzite CdMSe and zinc-blende CdMTe.

Conformations in CdMSe		Number of sites	Distance (Å)
I	(180°,180°)	6	8.6
II	(120°,180°)	6	8.2
III	(180°,120°)	6	8.2
IV	(180°,60°)+(180°,−60°)	3	7.5
V	(−60°,180°)+(60°,180°)	3	7.5
VI	(−60°,180°)+(−60°,−120°)	6	7.5
VII	(180°,−60°)+(−120°,−60°)	6	7.5
VIII	(180°,0°)	1	7.0
IX	(0°,180°)	1	7.0
X	(60°,60°)+(−60°,−60°)	3	6.1
XI	(−120°,60°)+(60°,60°)+(−60°,−60°)+(120°,−60°)	3	6.1

Conformations in CdMTe		Number of sites	Distance (Å)
(180°,180°)		12	9.2
(180°,60°), (180°,−60°)		12	7.9
(60°,180°), (−60°,180°)		12	7.9
(60°,60°), (−60°,−60°)		6	6.5

and the 11 NNN sets in the wurtzite structure. In part of the configurations two or four pathways are present simultaneously. The 11 sets of cadmiums are numbered from I to XI. The 11 types of cadmiums can result maximally in 11 THF shifted ^{113}Cd NMR lines with intensities proportional to the number of sites in each conformational set.

The NN superexchange integrals of Cd-based zinc-blende and wurtzite alloys $\text{Cd}_{1-x}\text{Mn}_x\text{Te}$, $\text{Cd}_{1-x}\text{Mn}_x\text{Se}$, and $\text{Cd}_{1-x}\text{Mn}_x\text{S}$ are all of the order of (7 ± 3) K.⁴ Shapira *et al.*¹⁷ have recently shown that in the wurtzite crystals the NN superexchange interactions between Mn ions occupying ‘‘in-plane’’ sites are different from those occupying ‘‘out-of-plane’’ sites. The direct Mn-Se-Mn bond conformation is identical for the in-plane and out-of-plane paramagnetic ion pairs, and it was argued that the differences in the NN superexchange constant result from differences between the additional polarization paths, involving four bonds. For example, the four-bond pathway Mn-Se-Cd-Se-Mn between the out-of-plane neighbors has a $(0^\circ, 60^\circ)$ or $(60^\circ, 0^\circ)$ conformation, while the pathway between in-plane neighbors is of the $(60^\circ, 60^\circ)$ type.

The spin polarization of the different path ways varies, yielding different superexchange constants. Since the THF interaction strength is also dependent on the polarization transfer through the bonds, the assignment of the bond conformations to the experimental THF coupling constants contributes to the understanding of the role of the path way in the superexchange interaction. Thus the objective of this study is to find the correlations between the THF coupling constants and the bond conformations in the wurtzite alloys.

In the following sections we discuss the magic angle spinning (MAS) ^{113}Cd NMR experiments on $\text{Cd}_{1-x}\text{M}_x\text{Se}$ alloys with various values of x at different temperatures and spin-

ning speeds of the samples. In Sec. II the sample preparation procedure is described and the parameters of the NMR experiments are given. In Sec. III the ^{113}Cd MAS NMR spectra of the $\text{Cd}_{1-x}\text{M}_x\text{Se}$ samples are presented and discussed, and in Sec. IV the results are summarized. As will be shown, an assignment of the spectral lines to the conformations I to XI can be made that is based on the analysis of the relaxation times and intensities of the lines.

II. EXPERIMENTAL DETAILS

A. NMR measurements

The NMR experiments were performed using a home-built 200-MHz NMR spectrometer, a Bruker 300-MHz CXP or a Bruker 300-MHz DSX NMR spectrometer. The Larmor frequencies of ^{113}Cd in these spectrometers are equal to 44.37 and 66.55 MHz, respectively. All measurements were performed on samples rotating in the external magnetic field at the magic angle. The spin-echo sequence $\{\pi/2-\tau-\pi-\tau\}$ -acquisition was used for the detection of the signals in all experiments. The length of the $\pi/2$ pulse varied from 3 to 4 μsec , and the delay time τ was always equal to the length of one rotor period. High-speed 5- and 7-mm and standard 7-mm MAS probes of Doty Scientific Inc. were used and the experiments were performed between 180 and 400 K. The spinning speeds of the samples varied from 2 to 7.5 kHz, with a stability of 30 Hz, and a Bruker variable-temperature unit W110512 provided a temperature stability of ± 0.2 K.

Spin-lattice relaxation times of ^{113}Cd nuclei were measured using the saturation recovery sequence $\{\pi/2-t\}_n-T-\pi/2-\tau-\pi-\tau$ -acquisition. In these experiments the amplitudes of the lines were monitored as a function of T and fitted to single exponents.

B. Sample preparation

$\text{Cd}_{1-x}\text{Mn}_x\text{Se}$, $\text{Cd}_{1-x}\text{Co}_x\text{Se}$, and $\text{Cd}_{1-x}\text{Fe}_x\text{Se}$ polycrystalline samples were prepared for x values between 0.003 and 0.05. First the $M\text{Se}$ binary compounds with $M = \text{Mn}, \text{Co},$ and Fe were synthesized. This was accomplished by mixing pure M and Se in a molar ratio of 1:1.1 and by evacuating the mixture in quartz ampoules to 10^{-5} Torr. The sealed ampoules were then heated at a rate of $50^\circ\text{C}/\text{h}$ up to 850°C and kept at that temperature for 3 days, after which they were annealed at 1000°C . The resulting $M\text{Se}$ compounds were mixed with CdSe in appropriate molar ratios, thoroughly milled in an agate mortar, and loaded into carbon-coated quartz ampoules. These ampoules were also sealed in a vacuum of 10^{-5} Torr and sintered at $1000\text{--}1100^\circ\text{C}$ for 10 days. To improve the homogeneity of the distribution of impurities for small x values ($x < 0.01$), the sintered polycrystalline ingots were milled and annealed a second time.

All samples were checked and characterized by energy-dispersive (x-ray fluorescence) spectroscopy (EDS) and by x-ray photoelectron spectroscopy (XPS). For our experiments we used only samples that were single-phase compounds with homogeneously distributed magnetic ions. The measured concentrations were in good agreement with those expected from the preparation procedure, their values varying by less than 5%.

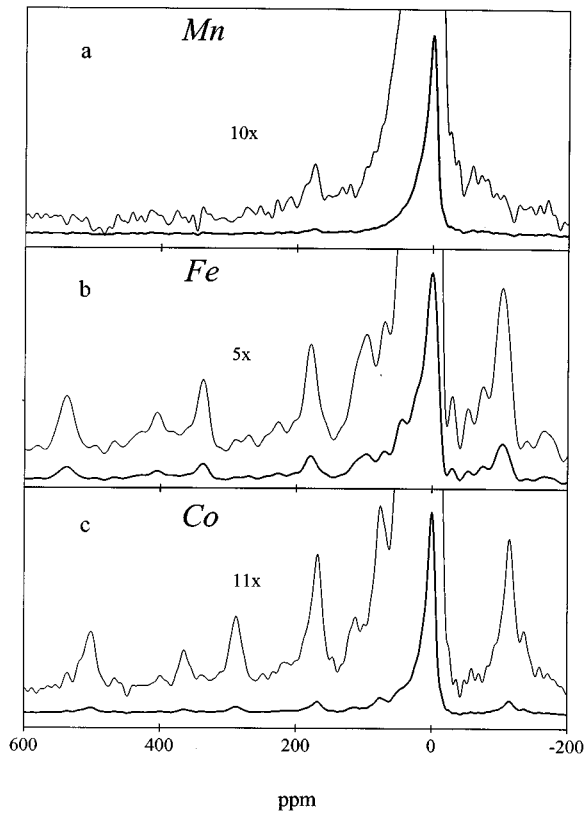


FIG. 1. ^{113}Cd MAS NMR spectra of the alloys (a) $\text{Cd}_{0.99}\text{Mn}_{0.01}\text{Se}$, (b) $\text{Cd}_{0.99}\text{Fe}_{0.01}\text{Se}$, and (c) $\text{Cd}_{0.99}\text{Co}_{0.01}\text{Se}$. The spectra are the Fourier transformation of the spin-echo signals, obtained at a spinning speed of 7.5 kHz and at a Larmor frequency of 44.37 MHz, after 3600 accumulations. The time between the rf pulses was 133 μsec and the repetition time was 15 sec. The 0 ppm positions were chosen at the maximums of the main CdSe lines. The low-intensity parts of the spectra are emphasized by multiplying the spectra by factors indicated in the figure.

III. NMR RESULTS

A. Spectral line positions

Figure 1 shows the ^{113}Cd MAS NMR spectra of the samples $\text{Cd}_{1-x}\text{Mn}_x\text{Se}$ for $x=0.01$, $\text{Cd}_{1-x}\text{Fe}_x\text{Se}$ for $x=0.01$, and $\text{Cd}_{1-x}\text{Co}_x\text{Se}$ for $x=0.009$. These results were obtained after Fourier transformation of the spin-echo signals of samples spinning at a rotor speed of 7.5 kHz. In these experiments 3600 echoes were accumulated with a repetition time of 15 sec. The spectra exhibit a set of low-intensity lines in addition to the main peaks. The main peak in each spectrum is located at the position of the ^{113}Cd line of pure CdSe and is chosen as the 0 ppm reference. The multifrequency spectral features were only obtained from Co and Fe samples; the Mn samples showed only a very small spectral line at 176 ppm in addition to the CdSe line. To assure that these differences did not depend on our synthesis, we performed ^{113}Cd NMR of $\text{Cd}_{1-x}\text{Mn}_x\text{Se}$ samples, not prepared by us.¹⁸ Also, in these samples no shifted ^{113}Cd lines were detected. The same is true in ^{113}Cd spectra of wurtzite $\text{Cd}_{1-x}\text{Mn}_x\text{S}$ alloys.¹⁹

Spin-echo experiments were repeated on $\text{Cd}_{1-x}\text{Co}_x\text{Se}$ samples, with $x=0.006$ and 0.009, with a repetition time of

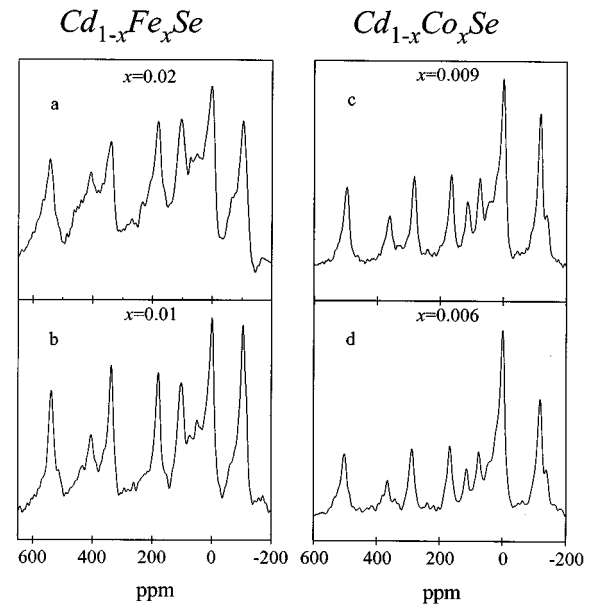


FIG. 2. ^{113}Cd MAS NMR spectra of the alloys (a) $\text{Cd}_{0.02}\text{Fe}_{0.98}\text{Se}$, (b) $\text{Cd}_{0.99}\text{Fe}_{0.01}\text{Se}$, (c) $\text{Cd}_{0.991}\text{Co}_{0.009}\text{Se}$, and (d) $\text{Cd}_{0.994}\text{Co}_{0.006}\text{Se}$. The experimental parameters of the measurements were the same as for Fig. 1, except that the repetition time of the experiments on the Fe alloys was 600 msec and of the Co alloys was 300 msec, and the number of accumulations was 24 000.

300 msec, and on $\text{Cd}_{1-x}\text{Fe}_x\text{Se}$ samples, with $x=0.01$ and 0.02, with a repetition time of 600 msec. Figure 2 presents the results of these experiments obtained after 24 000 accumulations. The spectral features of the Co and Fe samples are very similar, and the relative peak heights of the low-intensity lines of the two $\text{Cd}_{1-x}\text{Co}_x\text{Se}$ samples are about equal, as is the case for the $\text{Cd}_{1-x}\text{Fe}_x\text{Se}$ samples.

These results indicate that the low-intensity lines have shorter relaxation times than the main line and that their relative intensities seem to be independent of the concentration of the paramagnetic ions. Their intensities with respect to the main line increase for increasing x values. The difference between the spectra of the Mn and Co/Fe alloys could be due to a difference between the electronic relaxation times of these ions in the alloys. This possibility is discussed in the forthcoming text.

Following the previous ^{113}Cd NMR studies^{15,16} of alloys with a zinc-blende structure, we assumed that the shifted frequency bands correspond to the cadmium nuclei differently coordinated to the paramagnetic impurities. To demonstrate that the line shifts are governed by the THF interaction, we recorded ^{113}Cd spectra at different temperatures. Figure 3 illustrates the inverse temperature dependence of the shifts of six lines in the spectra of $\text{Cd}_{0.99}\text{Co}_{0.01}\text{Se}$ and $\text{Cd}_{0.99}\text{Fe}_{0.01}\text{Se}$. The shifts follow the Curie-Weiss law, confirming that they result from the hyperfine interaction between nuclear spins and paramagnetic ions.

At the high-temperature approximation ($B_0/T \ll 1$), the shift of each set of equivalent cadmium nuclei is given by

$$\Delta \nu_i = \left[\frac{A}{h} \right]_i \frac{g \mu_B S(S+1) B_0}{3k_B T} + \Delta \nu_{0i}, \quad (1)$$

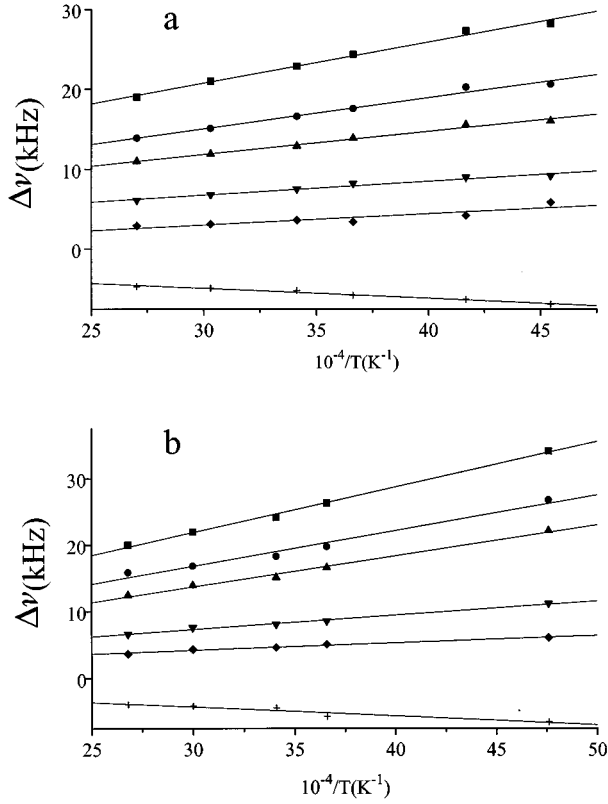


FIG. 3. Inverse temperature dependence of the shifts of six cadmium lines in the MAS spectra of (a) $\text{Cd}_{0.99}\text{Fe}_{0.01}\text{Se}$ and (b) $\text{Cd}_{0.99}\text{Co}_{0.01}\text{Se}$. The straight lines through the experimental points are least squares fits. The THF interaction constants in Table II were derived from the slopes of these lines.

where B_0 is the external magnetic field, $\Delta\nu_{0i}$ is the temperature-independent chemical shift contribution to $\Delta\nu_i$, and $[A/h]_i$ is the strength of the hyperfine interaction experienced by the i th set of cadmium nuclei. The values of the hyperfine coupling constants can be extracted from the slope of $\Delta\nu_i(1/T)$. Table II summarizes these values and the isotropic chemical shifts $\Delta\nu_{0i}$ of six lines in the $\text{Cd}_{0.99}\text{Co}_{0.01}\text{Se}$ and $\text{Cd}_{0.99}\text{Fe}_{0.01}\text{Se}$ alloys. These experiments were performed at a B_0 field of 4.7 T. The $[A/h]_i$ values were derived using g values of 2.29 (Ref. 20) and 2.3 (Ref. 10) and S values of 1.5 and 2 for Co^{2+} and Fe^{2+} , respectively. The absolute values of the THF coupling constants vary from 0.1 to 0.6 MHz. In the Fe alloys the chemical shift contributions are about zero, whereas in the Co alloys they follow the magnitudes of the hyperfine constants and vary from 120 to -30 ppm.

TABLE II. Transferred hyperfine interaction constants of $\text{Cd}_{1-x}\text{Fe}_x\text{Se}$ and $\text{Cd}_{1-x}\text{Co}_x\text{Se}$.

$\Delta\nu$ (ppm)	$\text{Cd}_{1-x}\text{Fe}_x\text{Se}$		$\Delta\nu$ (ppm)	$\text{Cd}_{1-x}\text{Co}_x\text{Se}$	
	A/h (MHz)	$\Delta\nu_0$ (ppm)		A/h (MHz)	$\Delta\nu_0$ (ppm)
544	0.47	29	515	0.58	118
423	0.37	14	367	0.43	74
348	0.32	-9	290	0.32	70
178	0.15	18	158	0.19	34
104	0.08	17	77	0.18	50
-102	-0.09	-3	-121	-0.13	-27

B. Relaxation time measurements

The spin-lattice relaxation rate of a cadmium spin belonging to the i th conformational set of cations has two contributions^{21,22}

$$\left[\frac{1}{T_1}\right]_i = \frac{2}{15} S(S+1) g^2 \mu_B^2 \gamma_I^2 \frac{1}{R_i^6} \left[\frac{3\tau}{1+(\omega_I\tau)^2} + \frac{7\tau}{1+(\omega_S\tau)^2} \right] + \frac{3}{2} S(S+1) \left[\frac{A}{h} \right]_i^2 \frac{\tau}{1+(\omega_S\tau)^2}. \quad (2)$$

The first term is due to fluctuations of the dipolar interaction between the magnetic moment of a paramagnetic ion and the nuclear cadmium spin, and the second term is due to the THF interaction. γ_I is the nuclear magnetogyric ratio, R_i is the distance between the paramagnetic ion and the cadmium atom in the i th configuration, τ is the electron spin-lattice relaxation time of the paramagnetic ion, ω_S is the electronic Larmor frequency, and ω_I is the nuclear Larmor frequency. In a field of 4.7 T we obtain that $\omega_I = 2.8 \times 10^8$ rad/sec and $\omega_S = 9.5 \times 10^{11}$ rad/sec, and for typical τ values²¹ of 10^{-12} – 10^{-11} sec for Co^{2+} and Fe^{2+} and 10^{-9} sec for Mn^{2+} , $\omega_I\tau < 1$ and $\omega_S\tau \gg 1$. For distances $R_{\text{NN}} = 4.3$ Å and $R_{\text{NNN}} = 6.1$ – 8.6 Å between a paramagnetic ion and its NN and NNN cadmium nuclei in the $\text{Cd}_{1-x}\text{M}_x\text{Se}$ crystal, respectively, the dipolar contributions to $1/T_1$ for the NN cadmium atoms in the Co and Fe alloys are of the order of 10^1 – 10^2 sec⁻¹ and for the NNN cadmium atoms 10^{-1} – 10 sec⁻¹. The largest THF contribution to the relaxation rate that can be expected, when we consider the largest hyperfine coupling constant A/h in Table II and a small τ value of 10^{-12} sec, is of the order of 1 sec⁻¹. From these considerations it follows that the main contribution to the $1/T_1$ value comes from its dipolar term.

T_1 relaxation times were measured by performing saturation recovery experiments. In Table III the experimental relaxation times of seven lines in the ^{113}Cd spectrum of $\text{Cd}_{0.994}\text{Co}_{0.006}\text{Se}$ are presented. They were derived from a single-exponential best-fitting procedure. In addition to the relaxation times, the relative line intensities of the fully relaxed spectrum were also obtained. The relaxation times of the lines at 77 and 115 ppm could not be determined and only an upper limit for their values can be given. These lines sit on top of a broad spectral feature, with a long spin lattice relaxation time, close to the main line of the spectrum.

The T_1 values vary between 100 and 600 msec. The line at 515 ppm with the largest A/h constant has a T_1 value of about 100 msec. If we assume that the relaxation time of that

TABLE III. Spin-lattice relaxation times and fully relaxed intensities of the ^{113}Cd lines of $\text{Cd}_{0.994}\text{Co}_{0.006}\text{Se}$ and the assignment of these lines to the sets of conformations I–XI with the number of sites and their theoretical T_1 relaxation times.

$\Delta\nu$ (ppm)	T_1 (msec) (experimental)	Intensities (arbitrary units)	Assignment	Total number of sites	T_1 (msec) (theoretical)
515	105 ± 15	55 ± 5	X+XI	6	103
367	135 ± 15	20 ± 3	VIII+IX	2	235
290	165 ± 40	64 ± 9	VII	6	356
158	325 ± 95	105 ± 15	V+VI	9	356
115	< 260	< 30	IV	3	356
77	< 600	< 100	I	6	809
-121	470 ± 100	150 ± 25	II+III	12	608

line is fully determined by the first term in Eq. (2) and that this line belongs to cadmium nuclei at distances $R_{\text{NN}} = 4.3 \text{ \AA}$ or $R_{\text{NNN}} = 6.1\text{--}8.6 \text{ \AA}$, then the correlation time τ becomes 2.6×10^{-12} sec or $2.2 \times 10^{-11}\text{--}1.8 \times 10^{-10}$ sec, respectively. For the same distances the τ value of the line at -121 ppm becomes 4.4×10^{-13} sec or falls in the range $3.6 \times 10^{-12}\text{--}2.9 \times 10^{-11}$ sec, respectively. In the next section we will show that the low-intensity lines correspond to NNN cadmium atoms. Therefore it seems right to conclude that the electronic relaxation time is about 2.5×10^{-11} sec.

There must exist a significant difference between at least part of the spectral parameters of the $\text{Cd}_{1-x}\text{Fe}_x\text{Se}$ and $\text{Cd}_{1-x}\text{Co}_x\text{Se}$ alloys and the $\text{Cd}_{1-x}\text{Mn}_x\text{Se}$ alloys. While the Co and Fe alloys exhibit a set of low-intensity lines, the Mn alloys for a variety of x values did not show any of these lines. A possible explanation for this difference may be that the T_2 values of the NNN cadmium nuclei in the Mn alloys are smaller than in the other alloys. The expression for the spin-spin relaxation rate of a cadmium spin contains a dipolar term and a term governed by the THF interaction, just as for $1/T_1$.^{21,22} The dipolar term of the i th configurational set has the form^{21,22}

$$\left[\frac{1}{T_2} \right]_i = \frac{\gamma_i^2 \gamma_S^2 h^2}{15R_i^6} S(S+1) \left\{ 4\tau + \frac{13\tau}{1 + (\omega_S\tau)^2} + \frac{3\tau}{1 + (\omega_I\tau)^2} \right\}. \quad (3)$$

According to this expression, the T_2 values of the NNN cadmiums in the Co alloys are in the range of 70–570 msec, when $\tau = 2.5 \times 10^{-11}$ sec. For the Mn alloys the spin-spin relaxation times become about 1–8 msec, when we assume that $\tau = 10^{-9}$ sec.²³ These values cannot be the reason for the disappearance of all the THF-shifted lines. Mn^{2+} electronic correlation times longer than 10^{-8} sec are necessary to explain the fact that the free induction decay signals of the THF-shifted cadmium nuclei are too short to be detected. In the case of the zinc-blende $\text{Cd}_{1-x}\text{Mn}_x\text{Te}$ alloys, the cadmium T_2 values are long enough to allow the observation of the THF shift lines.¹⁵ This fact may be related to the differences between the zinc-blende and wurtzite crystal structures.

C. Anisotropic contributions

To investigate which bond conformations cause the THF shifts in the cadmium spectra, we studied the MAS sideband patterns of the spectral lines as a function of the spinning

speed and the temperature. The relative intensities of the sidebands and center bands are influenced by the anisotropic parts of the chemical shift and the dipolar and THF interactions. Figure 4 shows two representative slow-spinning MAS spectra of $\text{Cd}_{0.994}\text{Co}_{0.006}\text{Se}$ obtained at different temperatures. The differences between these spectra indicate that the cadmium nuclei experience significant temperature-dependent anisotropic interactions. The relative contributions of the different interactions to the anisotropy are unknown. However, we will show that the dipolar contribution can provide us with the necessary information to conclude that the THF shifts in the spectra originate from interactions with NNN atoms.

Noting that the anisotropies of the different interactions have an additive effect on the sideband patterns, we shall restrict ourselves by considering only the dipolar contribution to the anisotropy. The value of the expected anisotropy of the dipolar interaction between a paramagnetic ion and a cadmium nucleus can be evaluated by calculating the high-temperature average magnetic moment of this ion,

$$\langle \mu \rangle = \frac{(g\mu_B)^2 S(S+1)}{3k_B T} B_0. \quad (4)$$

With $S = 1.5$ and $g = 2.29$ for Co^{2+} , the value of $\langle \mu \rangle$ becomes $0.104\mu_B$ in an external magnetic field of 7.05 T and at a temperature of 300 K. The dipolar anisotropy $\Delta\nu_{\text{dip}}$

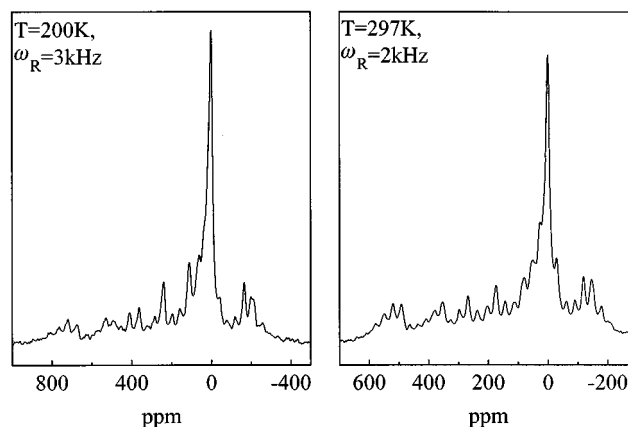


FIG. 4. Two typical slow spinning ^{113}Cd MAS NMR spectra of $\text{Cd}_{0.994}\text{Co}_{0.006}\text{Se}$. These spectra were obtained from experiment with a repetition time of 300 msec after 24 000 accumulations.

$= \gamma(\mu)R_{\text{NN}}^{-3}$ of a NN cadmium nucleus, interacting with a Co^{2+} at a distance $R_{\text{NN}}=4.3 \text{ \AA}$ in $\text{Cd}_{1-x}\text{Co}_x\text{Se}$, is 11.7 kHz. With the same parameters the dipolar anisotropy of a NNN cadmium nucleus at a distance of 6.1 Å from the Co^{2+} ion becomes 4.1 kHz. In the Fe alloys the dipolar anisotropies are somewhat larger.

We measured the sideband intensities of the various cadmium lines in $\text{Cd}_{0.994}\text{Co}_{0.006}\text{Se}$ as a function of temperature, spinning speed, and magnetic field (experiments were performed at 4.7 and 7.05 T). Spectral overlap of the sideband patterns, poor signal-to-noise ratios and the fact that at low temperatures the lines broaden significantly made it all difficult to perform an accurate Herzfeld-Berger analysis²⁴ of the MAS patterns. However, we were able to determine that the values of the anisotropy parameter $\Delta\nu_{\text{dip}}$ of all detectable sideband patterns were in the range of $4.8 \pm 2 \text{ kHz}$ at room temperature and $8.0 \pm 2.5 \text{ kHz}$ at $T=200 \text{ K}$. Because the experimental ^{113}Cd anisotropies of the $\text{Cd}_{1-x}\text{Co}_x\text{Se}$ alloys are clearly smaller than 11.7 kHz at room temperature and smaller than 17.5 kHz at $T=200 \text{ K}$, we must conclude that the THF-shifted lines correspond to NNN cadmium atoms. Almost all sideband patterns had an asymmetry parameter of about 0.1. The presence of the asymmetry indicates that the dipolar interaction is not the only contribution to the anisotropic parts of the spectra.

D. Line intensities

In order to make an assignment of the spectral lines in Figs. 1 and 2 and correlate them to the 11 sets of NNN conformations, the relative intensities of these lines in their fully relaxed spectrum must be compared with the number of cadmium atoms in each set (see Table I). In addition we expect that the values of the T_1 relaxation times of these lines are proportional to R_{NNN}^6 , according to the first term in Eq. (2). In Table III an assignment of the lines is suggested based on a comparison of the experimental line intensities and the magnitudes of their spin-lattice relaxation times with the numbers of cations in the conformational sets I–XI and their theoretical T_1 values, respectively. The theoretical T_1 's were calculated using the dipolar term of Eq. (2) with $\tau = 2.5 \times 10^{-11} \text{ sec}$ and the R_{NNN}^6 values of the assigned configurations. Realizing that the signal to noise of the spectra is rather poor and the fact that part of the spectral features overlap, the agreement between the experimental values and the calculated parameters is satisfactory. Most experimental

relaxation times are somewhat smaller than the theoretical ones, but their values follow the expected changes due to the changes in R_{NNN}^6 .

IV. SUMMARY

The presence of the paramagnetic ions in the CdSe DMS samples causes significant changes in the ^{113}Cd MAS NMR spectra. Well-resolved shifted lines with short relaxation times were observed in the Co- and Fe-based alloys. From the temperature studies and anisotropy measurements, we concluded that the shifts are caused by the THF interaction between the paramagnetic ions and their NNN cadmium nuclei. An assignment of the ^{113}Cd lines of $\text{Cd}_{0.994}\text{Co}_{0.006}\text{Se}$ to the sets of NNN cations with specific bond configurations was made by comparing experimental line intensities and relaxation times with the number of cations in these sets and their T_1 values calculated using their R_{NNN}^6 values. The strongest THF interaction occurs between a paramagnetic Co^{2+} and its NNN cations at a distance 6.1 Å and with a $(\pm 60^\circ, \pm 60^\circ) + (\pm 120^\circ, \pm 120^\circ)$ configuration. The value of the THF interaction is negative when the NNN cations are removed from the Co^{2+} ion by 8.2 Å and have a $(120^\circ, 180^\circ)$ bond configuration. The smallest value is found for the all-*trans* configuration. These results show the dependence of the THF coupling constants on the type of bond conformation. It is interesting to notice that there exists some correlation between the magnitudes of the THF constants and the distances between interacting spins. In future work the dependence of the THF interaction on these bond properties should be studied theoretically by evaluating the electronic spin polarizations in the crystal. Additionally, the values of the electronic correlation times in the different alloys should be evaluated in order to explain the relaxation data. The data presented in this paper can also be used as a tool for the determination of the incorporation of paramagnetic ions in DMS micro- and nanoparticles.

ACKNOWLEDGMENTS

The authors want to thank Professor W. Giriat for supplying DMS samples and Professor W. J. M. de Jonge and Dr. H. J. M. Swagten for stimulating discussions and advice regarding the analysis of our data. We wish to express our appreciation for the stimulating discussions with Dr. D. Zamir and his encouragement to continue the work. Part of this work was supported by the Minerva Foundation.

¹J. K. Furdyna and J. Kossut, *Semiconductors and Semimetals* (Academic, New York, 1988), Vol. 25.

²J. K. Furdyna, *J. Appl. Phys.* **64**, R29 (1988).

³S. Datta, J. K. Furdyna, and R. L. Gunshor, *Superlattices Microstruct.* **1**, 294 (1985).

⁴W. J. M. de Jonge and H. J. M. Swagten, *J. Magn. Magn. Mater.* **100**, 322 (1991).

⁵A. Mycielski, *J. Appl. Phys.* **63**, 3279 (1988).

⁶Y. Shapira, *J. Appl. Phys.* **67**, 5090 (1990).

⁷A. Mycielski, M. Arceszeska, W. Dobrowolski, C. Rigaux, A. Mauger, C. Telstelin, C. Julien, A. Lenard, M. Guillot, B. Wit-

kowska, and M. Menant, *Phys. Scr.* **T39**, 119 (1991).

⁸F. Hamdani, J. P. Lascaray, D. Coquillat, A. K. Bhattacharjee, M. Nawrocki, and Z. Golacki, *Phys. Rev. B* **45**, 13 298 (1992).

⁹H. Ehrenich, B. E. Larson, K. C. Hass, and A. E. Carlson, *Phys. Rev. B* **37**, 4137 (1988).

¹⁰A. Lewicki, J. Spalek, and A. Mycielski, *J. Phys. C* **20**, 2005 (1987).

¹¹S. P. McAlister, J. K. Furdyna, and W. Giriat, *Phys. Rev. B* **29**, 1310 (1984).

¹²R. R. Galazka, Shoichi Nagata, and P. H. Keesom, *Phys. Rev. B* **22**, 3345 (1980).

- ¹³J. Spalek, A. Lewicki, Z. Tarnawski, J. K. Furdyna, Z. Obszko, and R. R. Galazka, *Phys. Rev. B* **33**, 3407 (1988).
- ¹⁴A. Bruno and J. P. Lascaray, *Phys. Rev. B* **38**, 9168 (1988).
- ¹⁵K. Beshah, P. Becla, R. G. Griffin, and D. Zamir, *Phys. Rev. B* **48**, 2183 (1993).
- ¹⁶M. Gavish, S. Vega, and D. Zamir, *Phys. Rev. B* **48**, 2191 (1993).
- ¹⁷Y. Shapira, S. Foner, D. Heiman, P. A. Wolff, and C. R. McIntyre, *Solid State Commun.* **79**, 355 (1989); V. Bindilatti, T. Q. Vu, Y. Shapira, C. C. Agosta, E. J. McNiff, Jr., R. Kershaw, K. Dwight, and A. Wold, *Phys. Rev. B* **45**, 5328 (1992).
- ¹⁸Samples of CdMnS and CdMnS supplied by Professor W. Giritat from Centro de Fisica, Instituto Venezolano de Investigaciones Cientificas, Caracas 1020A, Venezuela were studied, for the comparison.
- ¹⁹Measurements performed on Cd_{0.99}Mn_{0.01}S and Cd_{0.97}Mn_{0.03}S at room temperature did not result in any shifted ¹¹³Cd lines.
- ²⁰N. Adachi, G. Kido, Y. Nakagawa, Y. Oka, and J. R. Anderson, *J. Magn. Magn. Mater.* **90&91**, 778 (1990).
- ²¹J. P. Jesson, in *NMR in Paramagnetic Molecules*, edited by G. N. Lamar, W. Den Horricks, Jr., and R. H. Holm (Academic, New York, 1973).
- ²²I. Solomon, *Phys. Rev.* **99**, 559 (1955).
- ²³C. P. Pool, Jr. and H. A. Farach, *Handbook of E.S.R.* (Academic Institute of Physics, New York, 1994).
- ²⁴J. Herzfeld and A. E. Berger, *J. Chem. Phys.* **73**, 6021 (1980).